# Influence of transitional volcanic strata on lateral diversion at Yucca Mountain, Nevada

Lorraine E. Flint and Alan L. Flint
Water Resources Division, U.S. Geological Survey, Sacramento, California, USA

John S. Selker
Department of Bioresource Engineering, Oregon State University, Corvallis, Oregon, USA

Received 5 June 2002; revised 14 October 2002; accepted 15 January 2003; published 3 April 2003.

[1] Natural hydraulic barriers exist at Yucca Mountain, Nevada, a potential high-level nuclear waste repository, that have been identified as possible lateral diversions for reducing deep percolation through the waste storage area. Historical development of the conceptual model of lateral diversion has been limited by available field data, but numerical investigations presented the possibility of significant lateral diversion due to the presence of a thin, porous rock layer, the Paintbrush nonwelded tuffs. Analytical analyses of the influence of transitional changes in properties suggest that minimal lateral diversion is likely at Yucca Mountain. Numerical models, to this point, have not accounted for the gradual transition of properties or the existence of multiple layers that could inadvertently influence the simulation of lateral diversion as an artifact of numerical model discretization. Analyses were made of subsurface matric potential measurements, and comparisons were made of surface infiltration estimates with deeper percolation flux calculations using chloride-mass-balance calculations and simulations of measured temperature profiles. These analyses suggest that insignificant lateral diversion has occurred above the repository horizon and that water generally moves vertically through the Paintbrush nonwelded tuffs. *INDEX TERMS:* 1875 Hydrology: Unsaturated zone; 5104 Physical Properties of Rocks: Fracture and flow; 1829 Hydrology: Groundwater hydrology; 5114 Physical Properties of Rocks: Permeability and porosity; *KEYWORDS:* volcanic tuffs, lateral diversion, capillary barrier, Yucca Mountain

**Citation:** Flint, L. E., A. L. Flint, and J. S. Selker, Influence of transitional volcanic strata on lateral diversion at Yucca Mountain, Nevada, *Water Resour. Res.*, *39*(4), 1084, doi:10.1029/2002WR001503, 2003.

## 1. Introduction

[2] Yucca Mountain, Nevada (Figure 1), is being studied to determine whether it is suitable for storage of high-level radioactive waste. The site was selected as a potential repository partially because of the abundance of natural barriers to the migration of water that could possibly interact with and corrode the waste canisters [*Roseboom*, 1983]. One of the natural barriers identified early in the characterization was the layered, nonwelded volcanic tuffs that exist between the ground surface and the potential repository horizon, and the potential of these tuffs to laterally divert water away from the waste storage area.

[3] The maintenance of a relatively dry subsurface is of utmost concern in waste containment. This situation can occur when no water penetrates the surface or when the infiltrating water is diverted laterally by way of a sloping permeability or capillary barrier, either natural or man-made. This paper presents an evaluation of the potential for lateral diversion by natural barriers.

[4] Waste containment is often a relatively small scale endeavor that is controlled by careful engineering. The situation at Yucca Mountain, on the other hand, is large scale, with the potential subsurface repository for high-level radioactive waste, extending over 4 $km^2$, at a depth in the unsaturated zone below ground surface of ~30 m. The initial investigations identified low precipitation (170 mm/yr) [*Hevesi et al.*, 1992] and natural geologic barriers (a deep unsaturated zone (500–1000 m) composed of Tertiary volcanic sequences of ash-flow and ash-fall tuffs with alternating layers of welded and nonwelded tuffs [*Buesch et al.*, 1996]) as critical attributes of the site. The highly fractured volcanic rocks surrounding the potential repository were expected to drain any percolating water quickly [*Roseboom*, 1983]. In addition, it was assumed, on the basis of early conceptual models, that water would be diverted laterally via the thin, sloping, high-permeability, nonwelded layer situated between the upper two thick, fractured, and welded units, the Tiva Canyon and Topopah Spring Tuffs [*Montazer and Wilson*, 1984; *Flint et al.*, 2001a] (Figure 2).

[5] Natural hydraulic diversion mechanisms may exist on large scales in deterministic depositional environments that provide large-scale features with contrasting hydrologic properties. The question posed here is whether an ash-flow/ash-fall tuff environment, such as that at Yucca Mountain, provides those features, and on a scale pertinent to the intent necessary at this site. The concept of a natural capillary barrier is summarized by *Montazer and Wilson* [1984] as a fine-grained layer overlying a coarse-grained layer, where water cannot flow from the smaller pores of the


0043-1397/03/2002WR001503

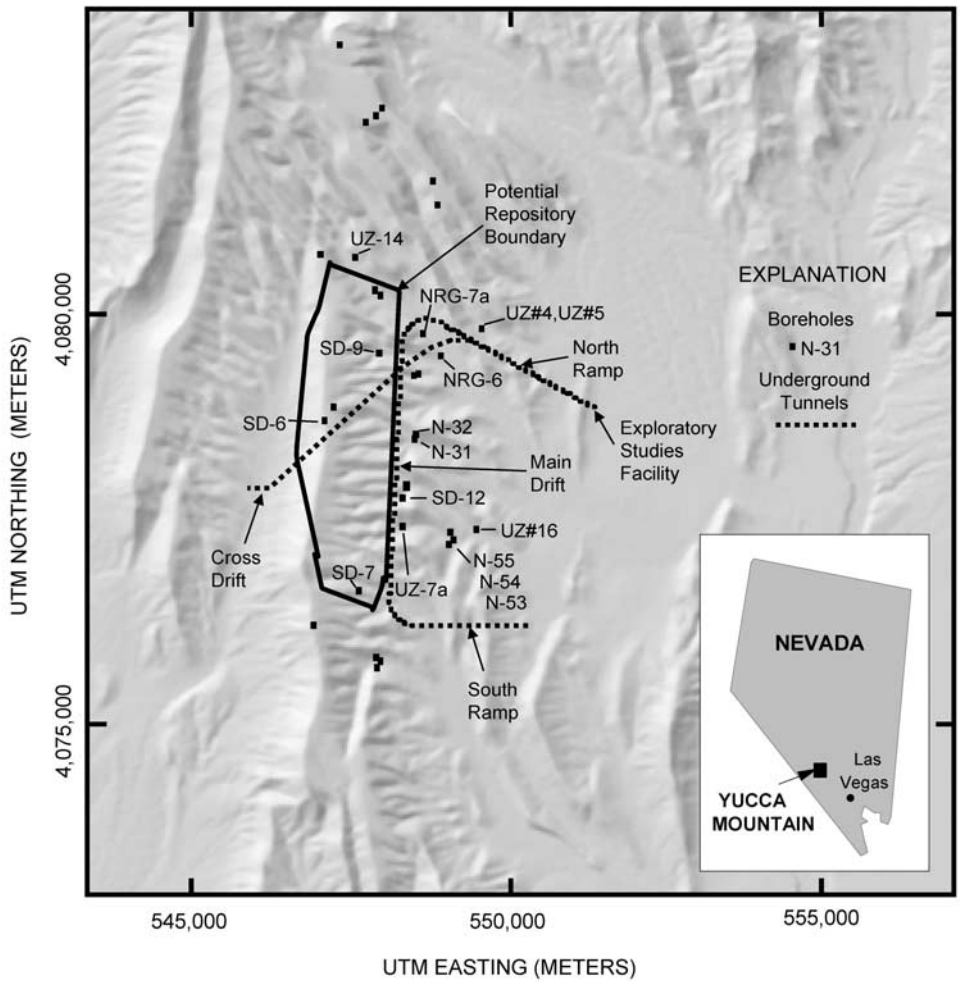


**Figure 1.** Location of study site, potential repository boundary, underground tunnels, and boreholes.

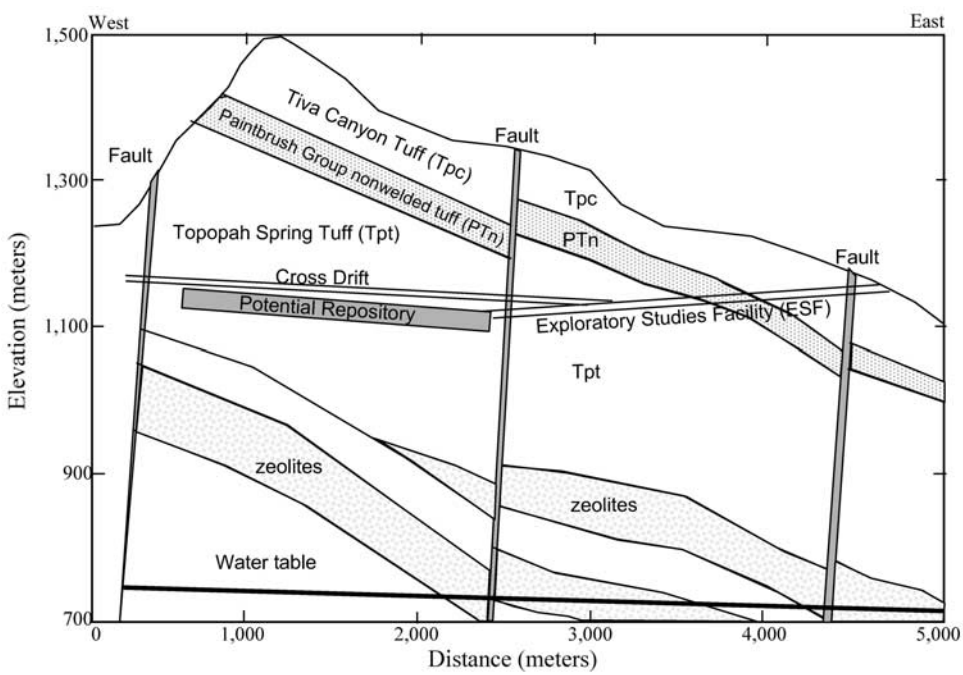


**Figure 2.** Cross-sectional schematic of major lithostratigraphic units at Yucca Mountain, and the locations of the potential repository, Exploratory Studies Facility, and Cross Drift. Scale is approximate with vertical scale 5 times the horizontal scale.

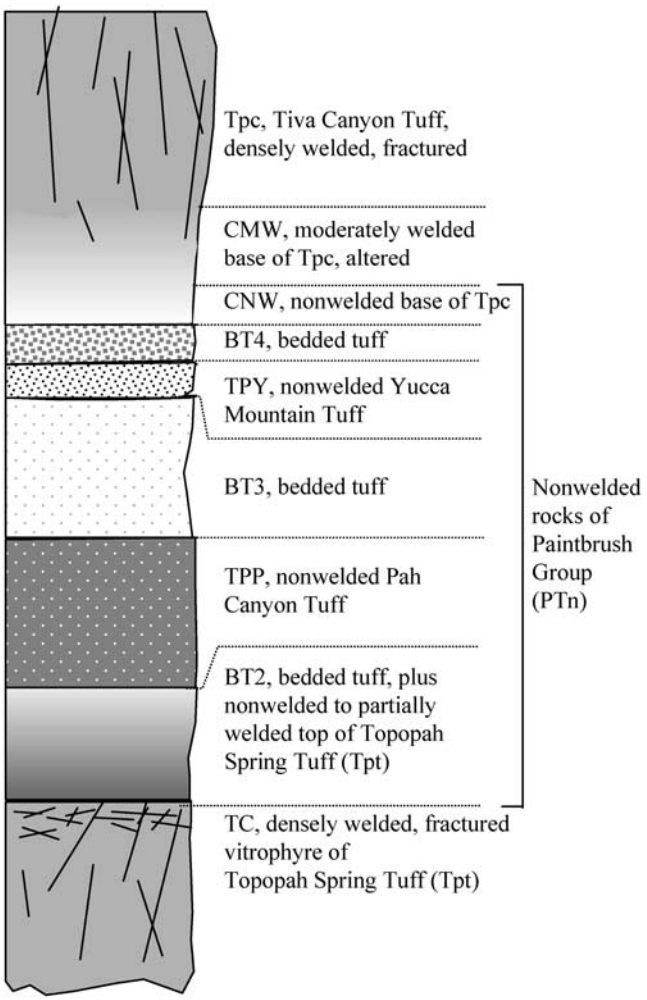


**Figure 3.** Lithostratigraphic schematic of the nonwelded rocks of the Paintbrush Group (PTn) and surrounding welded rocks, and hydrogeologic unit descriptions.

fine-grained layer into the larger pores of the coarse-grained layer until the height of water in the overlying layer exceeds a critical height, equivalent to the difference in the capillary rise (air-entry potential) of the two pore sizes. At Yucca Mountain, these definitions are complicated by the assumed flow mechanisms and must be carefully defined. Yucca Mountain consists of a series of fine- and coarse-grained rock layers (Figures 2 and 3), but for simplifying the definitions we assumed that a fine-grained, low-permeability rock (Tiva Canyon Tuff, Tpc) overlies a high-permeability, coarse-grained rock (nonwelded rocks of the Paintbrush Group, PTn), which, in turn, overlies a fine-grained, low-permeability rock (Topopah Spring Tuff, Tpt). If matrix flow is the only mechanism considered, as is more likely under conditions of very low net infiltration (that component of surface infiltration that makes it to a depth below which evapotranspiration processes can remove it), then a capillary barrier would exist at the interface between the fine-grained, high water-retention matrix of the Tpc and the coarse-grained PTn. The PTn has a low relative permeability for the range of negative water potentials likely to exist at low infiltration rates. In addition, a permeability barrier would exist between the base of the coarse-grained PTn and the fine-grained Tpt. In contrast, if flow though the fine-grained rock is predominantly through the fractures, as occurs at high net-infiltration rates, then the opposite scenario would apply. The high conductivity fractures in the Tpc overly a relatively lower permeability porous matrix (the PTn has few fractures) causing a permeability barrier at the base of the Tpc and the top of the PTn. A capillary barrier exists between the relatively lower permeability PTn and the higher-permeability fractures of the underlying Tpt (Figure 3).

[6] In fractured rock systems the amount of percolation can determine whether the flow is fracture- or matrix-dominated and hence whether the layer will act as a capillary barrier or a permeability barrier. Because of the variability in net infiltration at Yucca Mountain, both permeability and capillary barriers can be in effect at either the base of the Tpc or the base of the PTn. These conditions are further complicated by the degree of saturation of the matrix and the size of the fracture apertures and whether the fractures are open or filled.

[7] The purpose of this work is to evaluate evidence for a lack of lateral diversion on any significant scale at Yucca Mountain above the potential repository horizon. This will be done by discussing (1) how the conceptual model of subsurface flow that described the lateral diversion of water at Yucca Mountain changed over the years on the basis of an increase in available data and information, (2) how field data constrained calculations and numerical models describing lateral flow, (3) analytical calculations describing capillary barrier mechanisms on the basis of available properties from the site, and (4) data and interpretations representing various scales that support downward flow through the nonwelded layers and a lack of significant lateral diversion.

## 2. Historical Development of the Conceptual Model of Lateral Diversion at Yucca Mountain

### 2.1. Conceptual Model Development

[8] The original location for a potential repository in the unsaturated zone was first suggested by *Winograd* [1981]. Early project investigators had various views of the potential for lateral diversion. *Scott et al.* [1983] saw some potential for capillary barrier mechanisms to be effective at the contact of the upper welded unit, the Tiva Canyon Tuff (Tpc), and the underlying nonwelded tuffs of the Paintbrush Group (PTn), whereas *Roseboom* [1983] claimed no lateral component would exist because of the extensive fracture system. One year later, a conceptual model of flow at Yucca Mountain was published by *Montazer and Wilson* [1984] that included extensive discussions of capillary barrier mechanisms, and it was suggested that over 80% of the percolation (4 mm of the 4.5 mm/yr that they estimated) would be laterally diverted above and within the PTn. This was characterized as a large-scale process such as the scale depicted in Figure 2. *Sinnock et al.* [1987], *Klavetter and Peters* [1986], and *Peters and Klavetter* [1988] suggested the diversion would occur at the base of the PTn due to capillary barrier mechanisms because of the nonwelded tuff overlying even larger pores of the fractures in the densely welded Topopah Spring Tuff. *Wilson* [1996] stated that conventional wisdom still believed that the PTn acts as an effective capillary

barrier to divert much of the infiltrating water around the potential repository horizon, and, as recently as 1999, lateral flow in and above the PTn was still being included in the conceptual model of flow implemented in the three-dimensional site-scale flow model of Yucca Mountain [*Ritcey and Wu*, 1999; *Sonnenthal and Bodvarsson*, 1999].

### 2.2. Numerical Model Development

[9] Numerical models were used to test the hypotheses for lateral diversion using limited data and field observations in the late 1980s. *Rulon et al.* [1986] developed a two-dimensional (2-D) model that supported *Montazer and Wilson*'s [1984] concept of lateral flow in the PTn at low fluxes, with as much as 50% of the infiltrating water being diverted using fluxes of <1 mm/yr, but about 20% diverted at their maximum estimate of 4.5 mm/yr, considerably less than the nearly 90% suggested by *Montazer and Wilson* [1984].

[10] *Rockhold et al.* [1990] ran the first 3-D model in 1990 for a small portion of the site. It produced matrix flow in the PTn and diverted most of it laterally within the PTn. By 1995, many of the researchers still believed that lateral diversion in and above the PTn might reduce the volume of water that would penetrate the Topopah Spring Tuff, even though the estimates of potential net infiltration into the system had been increased from the earlier estimates of 1–5 mm/yr to an average of 5 mm/yr with a range of 0–80 mm/yr distributed spatially over the site [*Flint et al.*, 2001a, 2001b]. Although no significant or conclusive field evidence was available to support the concept of lateral diversion, several modeling exercises were done to test whether the available measured properties and geometry of the PTn could support or induce diversion [*Ho*, 1995; *Altman et al.*, 1996; *Moyer et al.*, 1996]. Typically, lateral diversion was attained, although minimally at high fluxes (>10 mm/yr). At lower fluxes (>0–5 mm/yr), the diverted water may have been an artifact of simplified geometry, unrealistic properties, the idealization of stratigraphic contacts as linear features, or a misrepresentation of the gradational nature of the transition of the Tiva Canyon Tuff into the nonwelded PTn. In 1999, water was diverted laterally above the PTn in the three-dimensional site-scale flow model of Yucca Mountain, developed by Lawrence Berkeley National Laboratory, a distance of ~250 m under current climate conditions, with a net-infiltration rate of 0–38 mm/yr [*Ritcey and Wu*, 1999], although they acknowledged that no field evidence of lateral diversion has been observed and suggested that faulting or interface heterogeneities limit lateral flow. Until only recently, there were no accurate and high-resolution matric-potential measurements of the subsurface rocks, particularly in the PTn, to test the model results. These measurements are now available for boreholes penetrating the PTn [*Flint et al.*, 2002b] and for locations along the extent of the Cross Drift [*Flint and Flint*, 2000].

### 2.3. Lithostratigraphic Description

[11] Early interpretations of lateral diversion were on the basis of several boreholes that provided geologic/lithologic descriptions and scanty measurements of hydrologic properties. Once more detailed information was available, such as detailed physical and hydraulic properties from core samples and geochemical data, more insightful models were developed to test the hypotheses of lateral diversion. Figure 3 schematically illustrates the generalized lithostratigraphy of the nonwelded PTn flanked above and below by the fractured, densely welded Tiva Canyon and Topopah Spring Tuffs. An example of the corresponding porosity and relative saturation of core samples from several boreholes is shown in Figure 4.

[12] The Paintbrush nonwelded hydrogeologic unit (PTn) of *Montazer and Wilson* [1984] is described as consisting of the nonwelded and partially welded base of the Tiva Canyon Tuff, the Yucca Mountain and Pah Canyon Tuffs, the upper nonwelded and partially welded upper part of the Topopah Spring Tuff, and the associated bedded tuffs. It consists of thin, nonwelded ash-flow sheets and bedded tuffs that thin to the southeast from a maximum thickness of ~200 m to a minimum of ~30 m in the vicinity of the potential repository.

[13] These rocks have been separated into several hydrogeologic units on the basis of lithostratigraphic description [*Moyer et al.*, 1996] and similarity in hydrologic properties [*Flint*, 1998, 2002]. The rocks near the base of the Tiva Canyon Tuff are characterized by a transition in porosity and mineral alteration and are divided into the CMW and CNW hydrogeologic units. The CMW hydrogeologic unit consists of moderately welded rocks near the base of the Tiva Canyon Tuff, with varying degrees of vapor phase corrosion that range from ~15% porosity at the top of the unit to >28% porosity at the bottom of the unit. The CNW consists of nonwelded to partially welded rocks at the base of the Tiva Canyon Tuff that range from >28% porosity to >50% porosity. The CMW and the top of the CNW in some boreholes consist of low permeability altered minerals with small pores and high water retention.

[14] The lithostratigraphic units of the PTn commonly are thin but distinct enough in properties to delineate as separate hydrogeologic units. A numerical modeling exercise was done by *Moyer et al.* [1996] to assess the hydrologic impact of these individual units and whether the mean properties of the units were different enough to maintain the individual layers as separate units. It was determined that abrupt and linear contacts, along with the contrasts in properties, were instrumental in creating lateral diversion along the sloping contacts. As an exercise, this indicated that the contrasts in the mean properties for each unit were different enough in most cases to maintain separate units. *Moyer et al.* [1996] suggested the possibility that the exercise simplified the linear character of the contacts. Field observations of outcrops and analyses of core data, such as in Figure 3, and sample properties as given by *Istok et al.* [1994], provide indications that these contacts are often only locally linear. Therefore they are less likely to divert water laterally because of heterogeneities that cause local increases in saturation that result in penetration across the boundary.

[15] The Yucca Mountain Tuff (TPY) has properties very similar to the BT4 and BT3 (Figure 3) and is absent in boreholes to the south of Drill Hole Wash (Figure 4, see boreholes N54 and N55), but has lower porosity and becomes moderately welded to the north (Figure 4, see borehole SD9). The nonwelded to partially welded Pah Canyon Tuff is hydrogeologic unit TPP. The bedded tuff BT2 and the nonwelded top of the Topopah Spring Tuff were not different

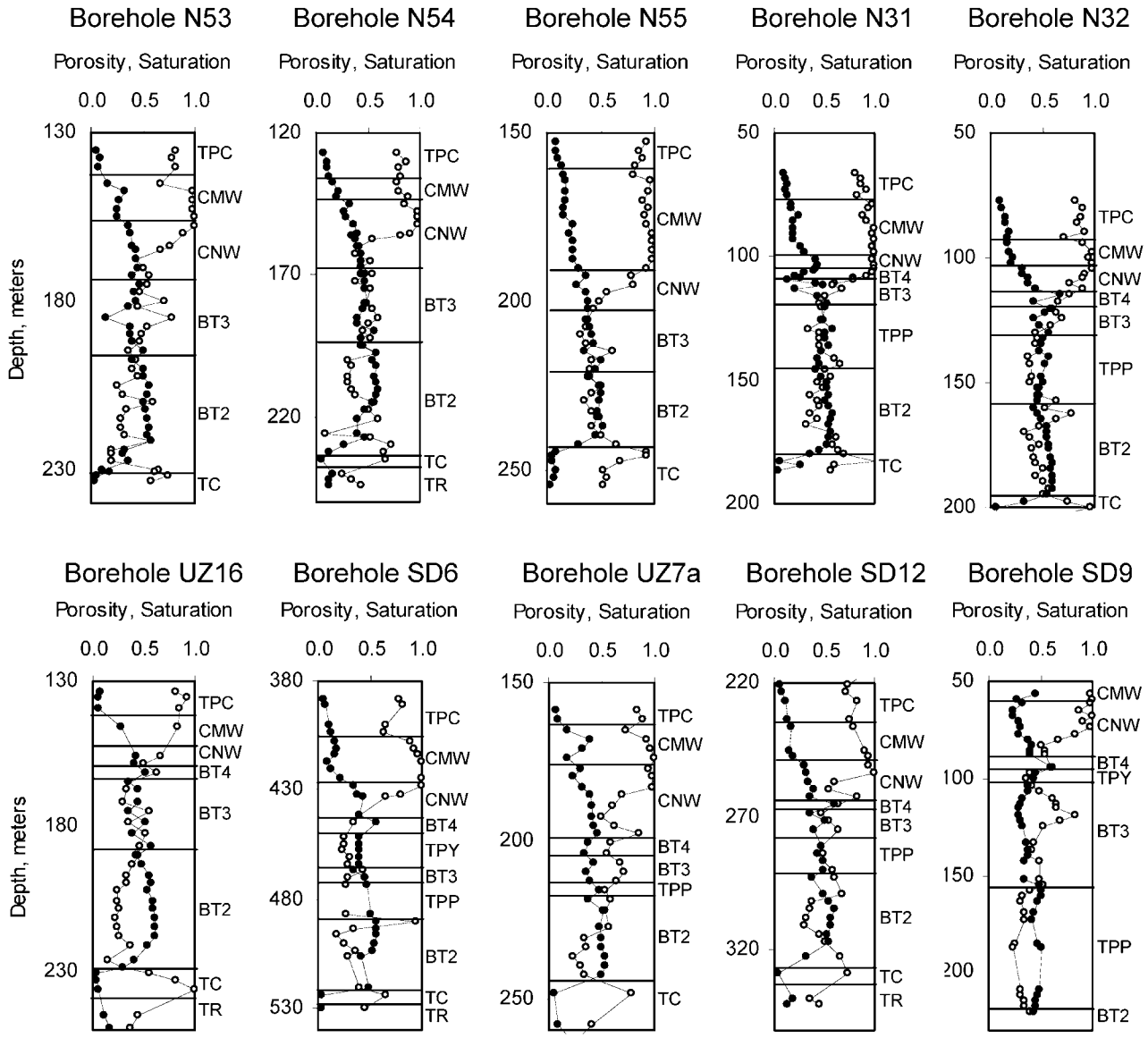


**Figure 4.** Porosity (solid circles) and saturation (open circles) for several boreholes penetrating through the nonwelded rocks of the Paintbrush Group (PTn).

enough in properties to maintain as separate units [*Moyer et al.*, 1996; *Flint*, 1998] and are represented by hydrogeologic unit BT2 (Figure 3). The nonwelded top of the Topopah Spring Tuff, encompassed by BT2, is a thin unit that transitions sharply from nonwelded to densely welded rock such that the borehole sample spacing of 0.8 m was not enough to adequately characterize the transition. Underlying this unit is a very thin, densely welded and fractured upper vitrophyre, hydrogeologic unit TC (Figure 3), which is typically <0.5 m thick, but varies from 0 to 2 m thick across Yucca Mountain. The TC typically has porosity <5% and has microfractures that have high permeability when saturated and very low permeability when unsaturated. This unit also has varying degrees of larger fractures that initiate just at the upper contact.

### 2.4. Evaluation of the Potential for Lateral Diversion From Field Data and Detailed Properties

[16] Borehole data of physical and hydraulic properties and water content collected from 1990 to 1995 provided support for the concept of a barrier (capillary or permeability), at least in some locations (Figure 4). These profiles of porosity and saturation suggest the possibility of barrier mechanisms operating because of the high saturations at the contacts between the CMW and the CNW, or the CNW and BT4, and the abrupt decline in saturation of the underlying rocks. The identification of high amounts of smectites in these locations further supported the concept (D. Bish, Los Alamos National Laboratory, written communication, 1992). The scenario suggests an initial depositional condition of a vapor phase corroded, moderately welded tuff with small pores with a gradational transition extending downward into a nonwelded tuff with larger pores that overlaid, with an abrupt contact, a bedded tuff with large pores. Given an effective barrier mechanism in this stratigraphic location, the development of long-term saturated conditions could alter the vitric rocks to montmorillonite, which is currently present. The presence of these altered minerals in the overlying rocks, however, greatly reduces

their permeability [*Flint*, 1998] so that they would drain only very slowly laterally down dip. This combined with a much lower air-entry potential and therefore thicker capillary fringe moves the barrier upward into the fractured welded rocks, through which the water could then drain laterally down dip. This is supported by the modeling exercise of *Moyer et al.* [1994] in which lateral diversion occurred primarily in high-conductivity fractures of the Tiva Canyon Tuff overlying the CMW. The mechanism, in this case, could be either a capillary barrier or a permeability barrier, depending on the flux mechanism (whether the percolation flux is dominated by flow through fractures or matrix). The locations of boreholes in which the altered minerals are the most developed are those in topographic positions most likely to have historically high surface fluxes, such as washes during the high-precipitation Holocene-age climate (Figure 4, UZ7a or N31) or where surface faulting exists (Figure 4, N55). As a result, this feature is not well developed in all boreholes.

[17] The collection of detailed rock properties provided information for detailed numerical modeling intended to test the effectiveness of the PTn to produce lateral diversion. The construction of numerical models typically relies on mean values of properties for a given lithostratigraphic unit, resulting in artificially abrupt contacts because of the manner in which gradational contacts between rock types are discretized, such as at the transition from welded to nonwelded rocks at the top of the PTn and the moderately welded to fractured rocks at the bottom of the PTn. In one case, *Kwicklis et al.* [1994] used porosity to estimate hydraulic properties, producing high-resolution changes in vertical property fields in two 1-D models of boreholes. The boreholes UZ4 and UZ5 (Figure 1) were located in a channel and an adjacent side slope. These models resulted in interpretations of lateral flow in the PTn from the channel borehole to the side slope borehole, but with a hesitancy to conclude anything more significant than subsurface spreading from a location with high surface fluxes such as this wash, which had significant runoff in recent years, to surrounding drier rocks.

[18] Larger-scale models consistently resulted in diversion [*Moyer et al.*, 1994; *Ho*, 1995; *Altman et al.*, 1995], particularly at the lower fluxes provided by the range of estimated net infiltration for the site. The use of properties that were stochastically distributed within hydrogeologic unit boundaries among grid cells on a fine scale, 2 cm $\times$ 4 cm, appeared to reduce the large-scale diversion by $\sim$15% [*Ho and Webb*, 1998]. This is probably the most realistic representation of the geometry and properties of the site.

[19] Properties and models have supported active barrier mechanisms and have provided support for lateral diversion. However, isotopic data, indicating young water, such as bomb-pulse chlorine-36 and tritium, in borehole samples from the PTn [*Civilian Radioactive Waste Management System* (*CRWMS*), 2000] indicate that not all water was laterally diverted above the nonwelded units and, indeed, that water did penetrate the potential barrier at the upper contact. These isotopes were later found extensively in the Topopah Spring Tuff in the Exploratory Studies Facility [*Fabryka-Martin et al.*, 1997], further confirming the notion of fast paths through the PTn. All measured bomb-pulse values were associated with faults that broke the continuity of the PTn. The extent of paths into and through the PTn is not completely known, however, and still does not preclude the notion of diversion because of the PTn.

## 3. Potential for Diversion Due to Natural Barriers

### 3.1. Analytical Evaluation of a Potential Capillary Barrier

[20] Analytical calculations can be made to evaluate the maximum potential for lateral diversion due to capillary barriers, assuming idealistic physical conditions. These calculations do not consider unsaturated flow phenomena such as fingering, or the spatial distribution of heterogeneities, that are likely to reduce diversion. This tool is therefore useful to assess when lateral diversion is unlikely to occur, given a specific set of hydraulic properties, and may help to ascertain the mechanisms contributing to apparent flow conditions in the unsaturated zone.

[21] *Ross* [1990] published analytical calculations of capillary barrier mechanisms leading to lateral diversion of water at sloping interfaces. The schematic represented in Figure 5 depicts the processes and variables used in his analysis. The analysis assumed rather idealized conditions to allow for the computation of lateral diversion of water. To describe media conductivity, Ross employed *Gardner*'s [1958] equation for conductivity:

$$K = K_s e^{\alpha\psi} \tag{1}$$

where $K$ is unsaturated hydraulic conductivity, $K_s$ is saturated hydraulic conductivity, $\alpha$ is a pore-size distribution index, and $\psi$ is water potential. The total horizontal flow, or maximum lateral diversion capacity ($Q_{\max}$), is a function of $K_s$, the angle of incline ($\varphi$), the applied vertical flux rate ($q$), and $\alpha$ for each of the two media on either side of the interface [*Ross*, 1990] with the lower layer indicated by the asterisk:

$$Q_{\max} = \frac{K_s \tan\varphi}{\alpha}\left[\left(\frac{q}{K_s^*}\right)^{\frac{\alpha}{\alpha^*}} - \left(\frac{q}{K_s}\right)\right]. \tag{2}$$

[22] *Ross* [1990] showed that to create a capillary barrier with significant diversion capacity, fine-textured media must overlie coarse-textured media with a linear, sloping contact, and a low flux rate. The barrier effect is overcome when the saturation is high enough in the overlying layer for the capillary pressure to be more than the underlying air-entry pressure. The barrier exists because of the difference in effective permeability between the fine layer and the coarse layer under unsaturated conditions. The length of diversion $L$ is a function of the upper layer only in the work by *Ross* [1990]:

$$L < \frac{K_s \tan\varphi}{\alpha q}. \tag{3}$$

[23] *Steenhuis et al.* [1991] extended this equation by making it a function of the air-entry pressure of the upper layer and the water-entry pressure (about equal to half the air-entry pressure) of the lower layer, which resulted in about twice the length of diversion. These calculations have

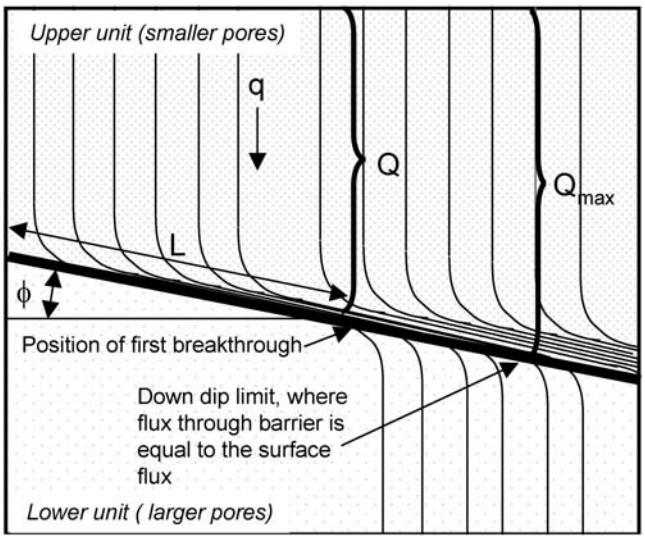


**Figure 5.** Schematic of analytical calculations of lateral diversion (modified from *Selker et al.* [1999, Figure 3.9]) where $Q$ is diversion capacity ($cm^2/d$), $Q_{max}$ is maximum diversion capacity ($cm^2/d$), $L$ is diversion length (cm), $q$ is applied flux (cm/d), $\phi$ is angle of incline, $\alpha$ is pore size indicator (1/cm) using *Gardner* [1958], and $K_s$ is saturated hydraulic conductivity (cm/d).

been shown to provide reasonable results in controlled laboratory experiments [*Walter et al.*, 2000].

[24] *Ross*'s [1990] equations assume an infinite thickness of the upper and lower layers isolating the interface from water potential gradient influences. This assumption is violated in gradational transitions depending on how the media geometry is represented. At Yucca Mountain the small pores of the altered, moderately welded Tiva Canyon Tuff have a very large air-entry value (calculated as $1/\alpha$), creating a saturated capillary fringe much thicker than the extent of the unit thickness, which averages about 2–9 m. *Ross* [1990] provides a simplified approximation for this case, which neglects the contrast with the lower layer and incorporates no influence of applied flux $q$ where $b$ is unit thickness:x

$$Q_{max} = K_s b \sin\varphi. \quad (4)$$

[25] However, as the pore size of the altered, moderately welded rocks is gradational with distance, there is no distinct upper bound to the layer. In essence, as the pores become smaller upward from the sloping interface, they provide a continuous water column and capillary fringe, until the height at which the transition is within the moderately welded to welded rocks and fractures are able to drain the accumulating water in the capillary fringe down dip. This conceptualization diffuses the clarity of the appropriate geometry or the most appropriate equation to use for calculations of $Q_{max}$, but supports the contention that either analytical calculation will serve as a maximum potential diversion.

[26] Several analyses were done to evaluate the maximum potential for lateral diversion by using equations (2) and (4) to calculate $Q_{max}$. Given the mean measured properties at this site, a 7-degree slope, the mean flux and range of fluxes, and the scale at which the geometry of features exist, several potential conditions are evaluated to assess the likelihood of any diversion extending beyond the dimensions of the potential repository, about a maximum of 1000 m down dip. In the following sections, four issues will be considered for analysis.

1. The first issue involves the upper transitional zone. Could there be lateral diversion within the transition of the CMW through the CNW? (1) What is the relation between number of layers used in the representation of the gradational system (corresponding to degree of contrast between adjacent layers) and the amount of diversion?, (2) how high must the saturated hydraulic conductivity be in the CMW to get appreciable diversion (conductivity is correlated to the development of alteration in the CMW)?, and (3) how low does the applied flux rate have to be for the given set of properties to predict significant lateral diversion?
2. The second issue involves an historical scenario. Could the conditions suggested in the historical scenario have sustained a capillary barrier to potentially result in the altered CMW, and how do the results compare with calculations of the existing transition?
3. The third issue involves the hydrogeologic units of the PTn. Are there any contrasts in properties of the units within the PTn that might produce lateral diversion?
4. The final issue involves the lower transitional zone. Is there a capillary barrier due to the position of the lower transition of the moderately welded Topopah Spring Tuff over an assumed range of fracture properties in TC?

#### 3.1.1. Upper Transitional Zone

[27] The first analysis to evaluate whether the CMW/CNW transition is effective in promoting lateral diversion is set up to test whether unrealistic contrasts in properties imposed by typical model development will result in inadvertent diversion. Average conditions and properties are used with a 9-m-thick unit that transitions from a porosity of 0.14 to 0.38. Values of $K_s$ and $\alpha$ are correlated with porosity [*Flint*, 2002] from measured data to provide realistic contrasts between the layers. Hydraulic conductivities for six of the different porosities are shown in Figure 6a. Computations of maximum expected lateral diversion $Q_{max}$ are made using equations (2) and (4) on the basis of an average flux of 5 mm/yr (0.00014 cm/d), encountering between two and 12 layers (Table 1). Qmax1 uses equation (2), which allows us to examine the relative maximum each layer could divert. Qmax2 is based on equation (4), assuming a limitation imposed by the layer thickness violates the assumptions for equation (2).

[28] An assessment of the relation of number of layers to calculated $Q_{max}$ shows that even though the two-layer system has the largest contrast in layer properties, the lower hydraulic conductivity of the layer with a porosity of 0.14 limits the lateral diversion (Table 1 and Figure 6b). The three-layer system has a somewhat less, but still large, contrast between two of the layers, but the higher hydraulic conductivity of the layer with a porosity of 0.26 allows much more lateral diversion. Reducing the contrast in $\alpha$ and $K_s$ by including additional layers reduces the diversion from this maximum for Qmax1.

[29] To evaluate the sensitivity of the parameters and the relation of $K_s$ and $q$ to $Q_{max}$, fluxes from 1 to 20 mm/yr

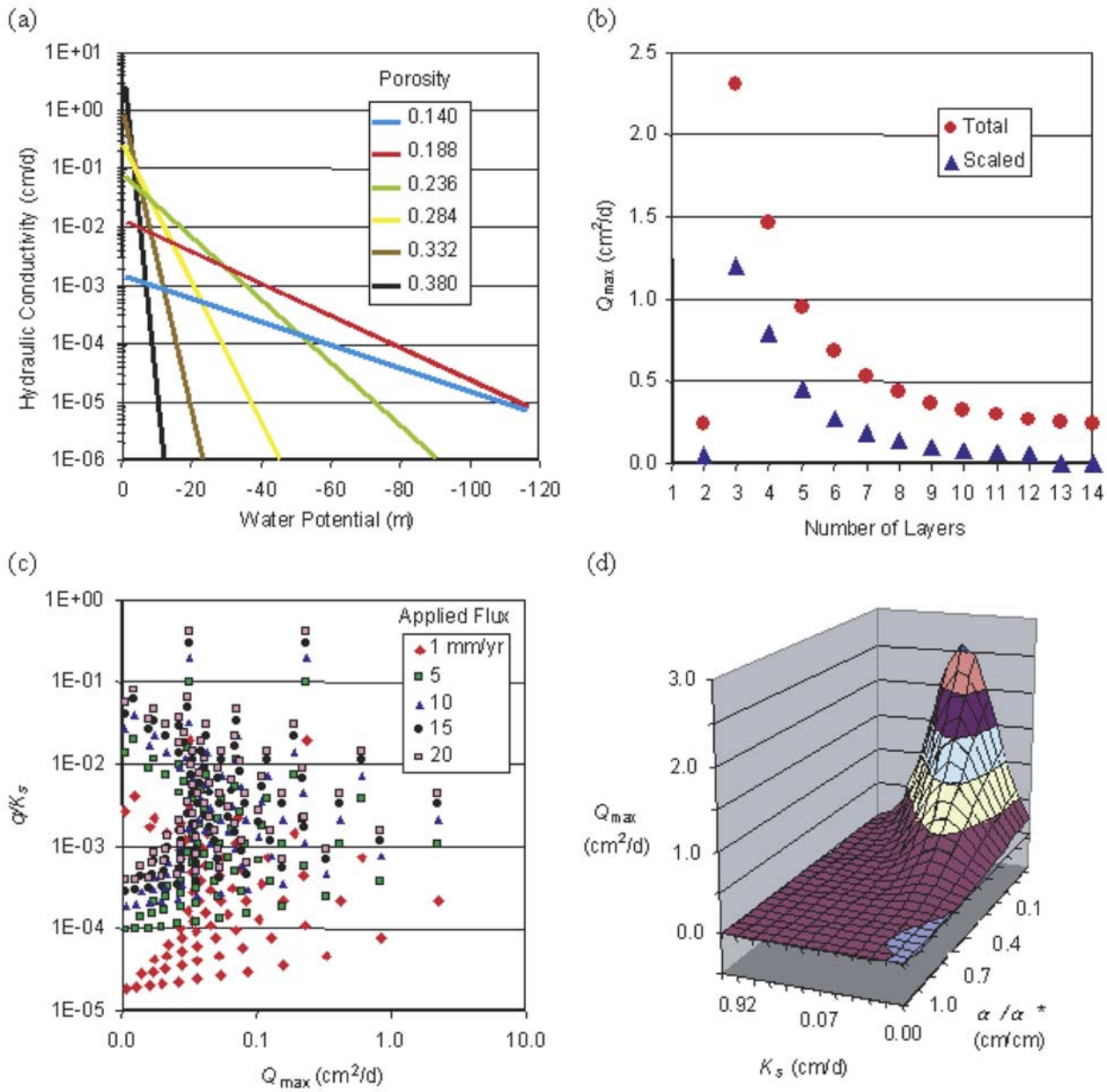


**Figure 6.** Data from calculations of lateral diversion potential $Q_{max}$ (a) hydraulic properties calculated for six porosities, (b) $Q_{max}$ calculated for systems with different numbers of layers, (c) $Q_{max}$ versus the ratio of $q$ to $K_s$ for five applied fluxes, and (d) $Q_{max}$ and the ratio of $\alpha$ for the upper layer ($\alpha$) to the lower layer ($\alpha$*) for a range of $K_s$.

were used to calculate $Q_{max}$. Figure 6c indicates that an optimum ratio of $q$ to $K_s$ of approximately 0.01 to 0.0001 results in the highest $Q_{max}$ (>2 cm$^2$/d) for the given set of properties. While the largest contrast possible in $\alpha$ for the two layers will produce the highest $Q_{max}$ (Figure 6d), there is an optimum $K_s$ for the given set of properties in Table 1. For example, for a flux of 0.5 mm/yr (0.00014 cm/d), a $K_s$ of near 0.1 cm/d results in the highest $Q_{max}$.

[30] Using the available analytical tools, we can also investigate diversion calculated assuming the most idealistic geometry exists, which provides the highest possible calculated $Q_{max}$. When equation (4) is used for Qmax2, which assumes the capillary fringe exceeds the layer thickness, the calculation is not limited by the upper boundary flux and the $Q_{max}$ is primarily a function of $K_s$, which is relatively high for more layers, nor is there any breakthrough into a lower layer. The calculation of Qmax2 assumes that the layer thickness is much less than $(\alpha \cos \varphi)^{-1}$, which is violated by most of the layers that have a thickness between 3% and 90% of the calculation of $(\alpha \cos \varphi)^{-1}$. There can be no direct comparison between Qmax1 and Qmax2, but they provide bounds for high and low diversion, given the possible interpretations of the physical system and the applicability of the assumptions.

[31] To produce a more realistic set of $Q_{max}$ values, Qmax1 (multiplying by layer thickness/air entry) was scaled to reflect the actual layer thickness that would provide a saturated capillary fringe flowing laterally down dip. These

**Table 1.** Calculations of Lateral Diversion Potential and Distance for a Sloping Interface[a]

| | | | | | | Qmax1 | | Qmax2 | | |
|---|---|---|---|---|---|---|---|---|---|---|
| | Porosity | Layer Thickness, cm | $\alpha$, $cm^{-1}$ | Air Entry, cm | $K_s$, cm/d | Per Layer | Total | Per Layer | Total | $L$, m |
| 2 layers | 0.14 | 450 | 0.0004 | 2278 | 0.001 | 0.2 | 0.2 | 0.1 | 0.1 | 17 |
| | 0.38 | 450 | 0.0124 | 80 | 2.069 | | | | | |
| 3 layers | 0.14 | 300 | 0.0004 | 2278 | 0.001 | 0.0 | 2.3 | 0.1 | 4.7 | 2 |
| | 0.26 | 300 | 0.0018 | 567 | 0.128 | 2.3 | | 4.7 | | 166 |
| | 0.38 | 300 | 0.0124 | 80 | 2.069 | | | | | |
| 4 layers | 0.14 | 225 | 0.0004 | 2278 | 0.001 | 0.0 | 1.5 | 0.0 | 11.1 | 0 |
| | 0.22 | 225 | 0.0009 | 1084 | 0.038 | 0.6 | | 1.0 | | 44 |
| | 0.30 | 225 | 0.0035 | 286 | 0.366 | 0.9 | | 10.0 | | 62 |
| | 0.38 | 225 | 0.0124 | 80 | 2.069 | | | | | |
| 5 layers | 0.14 | 180 | 0.0004 | 2278 | 0.001 | 0.0 | 0.9 | 0.0 | 16.1 | 0 |
| | 0.20 | 180 | 0.0007 | 1423 | 0.019 | 0.2 | | 0.4 | | 14 |
| | 0.26 | 180 | 0.0018 | 567 | 0.128 | 0.4 | | 2.8 | | 31 |
| | 0.32 | 180 | 0.0049 | 204 | 0.587 | 0.3 | | 12.9 | | 24 |
| | 0.38 | 180 | 0.0124 | 80 | 2.069 | | | | | |
| 6 layers | 0.14 | 150 | 0.0004 | 2278 | 0.001 | 0.0 | 0.7 | 0.0 | 19.9 | 0 |
| | 0.19 | 150 | 0.0006 | 1634 | 0.012 | 0.1 | | 0.2 | | 5 |
| | 0.24 | 150 | 0.0012 | 846 | 0.063 | 0.2 | | 1.2 | | 16 |
| | 0.28 | 150 | 0.0027 | 375 | 0.245 | 0.2 | | 4.5 | | 17 |
| | 0.33 | 150 | 0.0059 | 168 | 0.769 | 0.2 | | 14.1 | | 11 |
| | 0.38 | 150 | 0.0124 | 80 | 2.069 | | | | | |
| 8 layers | 0.14 | 113 | 0.0004 | 2278 | 0.001 | 0.0 | 0.4 | 0.0 | 25.1 | 0 |
| | 0.17 | 113 | 0.0005 | 1861 | 0.007 | 0.0 | | 0.1 | | 1 |
| | 0.21 | 113 | 0.0008 | 1274 | 0.025 | 0.1 | | 0.3 | | 5 |
| | 0.24 | 113 | 0.0013 | 756 | 0.078 | 0.1 | | 1.1 | | 8 |
| | 0.28 | 113 | 0.0024 | 422 | 0.205 | 0.1 | | 2.8 | | 8 |
| | 0.31 | 113 | 0.0042 | 236 | 0.481 | 0.1 | | 6.6 | | 6 |
| | 0.35 | 113 | 0.0074 | 135 | 1.034 | 0.1 | | 14.2 | | 4 |
| | 0.38 | 113 | 0.0124 | 80 | 2.069 | | | | | |
| 10 layers | 0.14 | 90 | 0.0004 | 2278 | 0.001 | 0.0 | 0.3 | 0.0 | 28.4 | 0 |
| | 0.17 | 90 | 0.0005 | 1975 | 0.005 | 0.0 | | 0.1 | | 0 |
| | 0.19 | 90 | 0.0006 | 1541 | 0.015 | 0.0 | | 0.2 | | 2 |
| | 0.22 | 90 | 0.0009 | 1084 | 0.038 | 0.1 | | 0.4 | | 4 |
| | 0.25 | 90 | 0.0014 | 710 | 0.087 | 0.1 | | 1.0 | | 5 |
| | 0.27 | 90 | 0.0022 | 451 | 0.185 | 0.1 | | 2.0 | | 4 |
| | 0.30 | 90 | 0.0035 | 286 | 0.366 | 0.0 | | 4.0 | | 4 |
| | 0.33 | 90 | 0.0055 | 183 | 0.683 | 0.0 | | 7.5 | | 3 |
| | 0.35 | 90 | 0.0083 | 120 | 1.214 | 0.0 | | 13.3 | | 2 |
| | 0.38 | 90 | 0.0124 | 80 | 2.069 | | | | | |
| 12 layers | 0.14 | 75 | 0.0004 | 2278 | 0.001 | 0.0 | 0.2 | 0.0 | 30.7 | 0 |
| | 0.16 | 75 | 0.0005 | 2042 | 0.004 | 0.0 | | 0.0 | | 0 |
| | 0.18 | 75 | 0.0006 | 1708 | 0.010 | 0.0 | | 0.1 | | 1 |
| | 0.21 | 75 | 0.0008 | 1328 | 0.023 | 0.0 | | 0.2 | | 2 |
| | 0.23 | 75 | 0.0010 | 971 | 0.048 | 0.0 | | 0.4 | | 3 |
| | 0.25 | 75 | 0.0015 | 682 | 0.094 | 0.0 | | 0.9 | | 3 |
| | 0.27 | 75 | 0.0021 | 470 | 0.173 | 0.0 | | 1.6 | | 3 |
| | 0.29 | 75 | 0.0031 | 323 | 0.306 | 0.0 | | 2.8 | | 3 |
| | 0.31 | 75 | 0.0045 | 224 | 0.518 | 0.0 | | 4.7 | | 2 |
| | 0.34 | 75 | 0.0064 | 157 | 0.846 | 0.0 | | | | |
| | 0.36 | 75 | 0.0090 | 111 | 1.341 | 0.0 | | | | |
| | 0.38 | 75 | 0.0124 | 80 | 2.069 | | | | | |

[a]A slope of 7 degrees is used with an applied flux of 0.5 mm/yr. Qmax1 is diversion potential using equation (2), Qmax2 uses equation (4) for a layer with an upper boundary, and $L$ is calculated as Qmax1 divided by the applied flux.

resulting values are 20–50% lower than Qmax1 (Figure 6b). Regardless of the assumptions for the calculations of $Q_{max}$, they represent the highest realistic potential for lateral diversion in this gradational unit transitioning from the welded rocks to the nonwelded rocks (Table 1), and yet they show virtually no lateral diversion when the system is discretized to include more than about five layers in 9 m of thickness.

[32] In equation (3), *Ross* [1990] assumes that the pore size distribution index $\alpha$ provides an estimate for the capillary fringe height, which is necessary for calculating diversion length $L$. The assumption of an infinite upper boundary distance is violated for our purposes; estimates of $L$ can be simplified by dividing Qmax1 (in $cm^2$/d) by $q$ (in cm/d) to attain $L$ (in cm). These results (Table 1) indicate that water is not diverted laterally distances that approach the dimensions of the potential repository. The distances are insignificant when the system is discretized to include more than six layers, but even the greatest distance of 166 m in the three-layer system is relatively inconsequential considering the scale of the repository.

### 3.1.2. Historical Scenario

[33] To evaluate a historical scenario prior to the extensive mineral alteration of the base of the Tiva Canyon Tuff, a surrogate set of properties is considered. The top of the Tiva Canyon Tuff has a somewhat parallel development to that of the bottom, with similar welding due to cooling rate, and vapor phase corrosion influencing the porosity. While the upper part is crystal rich, rather than crystal poor, there

**Table 2.** Mean Values and Standard Deviations for Measured Core Properties, Compiled From All Boreholes for Each Hydrogeologic Unit[a]

| Hydrogeologic unit | Porosity (v/v) | | Saturation | | | Saturated Hydraulic Conductivity, m/s | | | Moisture-Retention Curve-Fit Parameters[b] | | | | Fracture Density (F/m) |
|---|---|---|---|---|---|---|---|---|---|---|---|---|---|
| | Mean | Standard Deviation | Mean | Standard Deviation | N | Geometric Mean | Standard Deviation | N | $\alpha$, $MPa^{-1}$ | n | m | N | |
| CW | 0.08 | 0.03 | 0.80 | 0.14 | 616 | 5.7E-12 | 3.4E-11 | 16 | 2.8 | 1.20 | 0.17 | 9 | 5.0 |
| CMW | 0.20 | 0.05 | 0.91 | 0.13 | 96 | 1.8E-10 | 1.3E-07 | 5 | 0.3 | 1.35 | 0.26 | 3 | 1.0 |
| CNW | 0.39 | 0.07 | 0.69 | 0.24 | 105 | 1.2E-08 | 1.1E-05 | 10 | 96.2 | 1.19 | 0.16 | 6 | 0.5 |
| BT4 | 0.44 | 0.12 | 0.51 | 0.20 | 34 | 5.8E-07 | 2.1E-03 | 4 | 53.3 | 1.21 | 0.18 | 7 | 0.5 |
| TPY | 0.27 | 0.09 | 0.64 | 0.23 | 48 | 1.6E-07 | 7.8E-06 | 3 | 162.6 | 1.25 | 0.20 | 3 | 1.0 |
| BT3 | 0.41 | 0.08 | 0.53 | 0.16 | 87 | 5.4E-07 | 1.4E-06 | 17 | 93.2 | 1.16 | 0.14 | 5 | 0.5 |
| TPP | 0.50 | 0.04 | 0.36 | 0.13 | 166 | 9.3E-07 | 4.4E-07 | 11 | 47.2 | 1.36 | 0.26 | 2 | 1.0 |
| BT2 | 0.49 | 0.10 | 0.39 | 0.15 | 177 | 2.2E-06 | 9.4E-06 | 21 | 51.4 | 1.23 | 0.19 | 7 | 0.5 |
| TC | 0.05 | 0.04 | 0.63 | 0.17 | 72 | 1.6E-09 | 2.6E-07 | 5 | 1.5 | 1.27 | 0.21 | 3 | 25.0 |

[a]N, number of samples; MPa, megapascals; F/m, fractures per meter; v/v, dimensionless volume.
[b]Moisture-retention curve-fit parameters determined using *van Genuchten* [1980].

are similarities in hydrologic properties [*Flint*, 2002]. If the properties of the crystal-rich moderately welded rock ($\alpha$ = 0.0012 $cm^{-1}$, $K_s$ = 0.138 cm/d) are used to overly the CNW, the $Q_{max}$ is 46 $cm^2$/d compared with 0.24 $cm^2$/d in the existing rocks. This suggests that capillary conditions are viable to creating saturated conditions conducive to mineral alteration in vitric rocks. Once the minerals are altered, the rocks then maintain high saturation due to moisture-retention characteristics.

[34] This evaluation provides credence to the early conceptual models that were based on minimal rock property data and general lithostratigraphic descriptions. It was not until detailed information, including measurements of the properties and mineral alteration of the gradational transition, was available that this conceptual model would lose its viability.

### 3.1.3. Hydrogeologic Units of the PTn

[35] Early conceptual models also suggested that lateral diversion occurred within the layers of the PTn because of the apparent linearity of the contacts over long distances. It was assumed that the properties were similar spatially within the units as the deterministic depositional processes governed their features [*Rautman and Flint*, 1992; *Istok et al.*, 1994; *Flint et al.*, 1996]. Mean properties for the nonwelded ash-fall and bedded tuff layers in the PTn are relatively similar, but with large variability over the site (Table 2). This spatial variability was confirmed by *Istok et al.* [1994], *Moyer et al.* [1996], and *Flint* [1998, Table 8]. Generally the units within individual boreholes because of the nature of the depositional process do not have abrupt changes in properties (Figure 4). However, calculations could be made using the specific properties for any given borehole and get widely variable results. Calculated lateral diversion $Q_{max}$ from the mean values results in about 4 $cm^2$/d for the contrast between BT4 and TPY and no diversion for the contrasts between the other adjacent units, even within the ranges of their variance. (The TPY only exists north of the potential repository location and thus is not very relevant to the consideration of lateral diversion above the repository.) The key here is that the lateral variability between boreholes is high enough that lateral diversion is very unlikely to extend any distance within the PTn units. This is particularly evident on the basis of the fracturing in the units (Table 2) and faults that result in small offsets that interrupt the linear continuity [*Heiberger*, 1996]. The fracture density for the PTn hydrogeologic units is one fracture every 1–2 m, and while these fractures are not likely to result in offsets creating contrasts in properties, they are likely to conduct water faster than the matrix. The consequences of the faults that break the PTn are evident on the basis of numerous measurements of bomb-pulse chlorine-36 in the Exploratory Studies Facility (ESF) [*Fabryka-Martin et al.*, 1997]. These measurements indicate that not only are there breaks in the PTn, but continuous fracture paths extend from the surface through the PTn to the ESF in many locations. The presence of bomb-pulse chlorine-36 indicates the presence of water that is less than about 50 years in age, inferring that a fast path for the water to percolate through the PTn must exist. The frequent spacing of these bomb-pulse chlorine-36 measurements in the ESF supports the conceptual model of the PTn, which notes that it is broken by faults and does not have the lateral continuity necessary for large-scale diversion.

[36] One approach to analyzing the variability in the units and therefore the varying contrasts between the layers, is to stochastically distribute the properties in each unit using the mean and variation for each unit and to evaluate the range in contrasts at the boundaries between units. Modeling exercises have investigated diversion using this approach with resulting declines in diversion in comparison to a simple layered approach to distributing the properties [*Altman et al.*, 1995; *Ho and Webb*, 1998].

### 3.1.4. Lower Transitional Zone

[37] The base of the PTn is the final avenue for lateral diversion above the potential repository horizon. This transition ranges from a porosity of about 0.4–0.05 or less over a distance of about 1–2 m. The porosity transition within the BT2 is smooth; however, the contact with the vitrophyre, TC, which has many very small to relatively large fractures, is very abrupt. The analysis, in this case, is not as in the transitional example, but considers two-layer scenarios. Properties for fractures of specific apertures were modeled by *Kwicklis and Healy* [1993] and are used in this analysis. To derive $\alpha$ values for the calculations, a correlation of $\alpha$ using *Gardner* [1958] and $\alpha$ from *van Genuchten* [1980] were made on the basis of 18 samples from those used to calculate the mean values in Table 2, which represented the range of units from welded to nonwelded

**Table 3.** Properties for Calculation of Lateral Diversion Potential and Length of Lower Paintbrush Tuff Nonwelded Transition Into Topopah Spring Tuff Welded Rocks[a]

| | Matrix Porosity (v/v) | Fracture Aperture,[b] microns | Gardner α, $cm^{-1}$ | $K_s$, cm/d | Air Entry, cm | Total Qmax, $cm^2/d$ | $L$, m |
|---|---|---|---|---|---|---|---|
| Vitric tuff | 0.2 | | 0.0007 | 1.9E-02 | 1423 | 2.8 | 207 |
| Fractures | | 25 | 0.0248 | 1.8E-02 | 40 | | |
| Vitric tuff | 0.2 | | 0.0007 | 1.9E-02 | 1423 | 3.2 | 230 |
| Fractures | | 125 | 0.1482 | 2.7E-01 | 7 | | |
| Vitric tuff | 0.1 | | 0.0004 | 1.2E-04 | 1423 | 0 | 0 |
| Fractures | | 25 | 0.0248 | 1.8E-02 | 40 | | |
| Vitric tuff | 0.1 | | 0.0004 | 1.2E-04 | 2465 | 0 | 0 |
| Fractures | | 125 | 0.1482 | 2.7E-01 | 7 | | |
| Vitric tuff | 0.05 | | 0.0004 | 7.2E-07 | 2499 | 0 | 0 |
| Fractures | | 25 | 0.0248 | 1.8E-02 | 40 | | |
| Vitric tuff | 0.05 | | 0.0004 | 7.2E-07 | 2499 | 0 | 0 |
| Fractures | | 125 | 0.1482 | 2.7E-01 | 7 | | |

[a]$K_s$, saturated hydraulic conductivity; $Q_{max}$, diversion potential; $L$, length; v/v, dimensionless volume; cm, centimeters; m, meters.
[b]Fracture properties from *Kwicklis and Healy* [1993].

for which curve-fit parameters were estimated using both equations. The correlation had an $R^2$ of 0.89.

[38] Properties for nonwelded tuff of three porosities were used to overlie fractures of two apertures (Tables 3 and 4). As the contrast between α is high for all sets of layers, the $K_s$ is the limiting factor in the upper layer for the 0.1 and 0.05 porosity rocks. The layers with porosities of 0.05 and 0.1 have zero diversion length and no diversion capacity, whereas the layer with a porosity of 0.2 has a potential diversion of greater than 200 m. The difference in fracture aperture makes little difference in the calculation of $Q_{max}$ or $L$. These results show the importance of accurately representing the upper layer properties in the calculation of lateral diversion at this transitional boundary. They support the contention that lateral diversion caused by a capillary barrier in this transitional zone is insignificant when the system geometry is realistically represented.

### 3.2. Evaluation of Large-Scale Lateral Diversion

[39] Large-scale water flow processes can be investigated using measurements of rock samples collected from surface-based boreholes or subsurface excavations, or monitoring of moisture conditions in deep boreholes within subsurface excavations. These measurements represent vertically and laterally integrated subsurface conditions at various scales [*Flint et al.*, 2002b] and assist in the evaluation of processes operating at the scale of the potential repository. The analyses of these data lend evidence of generally vertical flow through the PTn whether via fast paths or through the matrix. These apparently dominant processes do not reduce the amount of water percolating through the repository horizon.

#### 3.2.1. Subsurface Collection of In Situ Water Potential Data

[40] To evaluate large-scale lateral diversion, Darcy's law was used to calculate the lateral flux downslope between two boreholes drilled vertically penetrating the PTn and the upper rocks of the welded Topopah Spring Tuff (Figure 7). This method uses estimates or measurements of hydraulic conductivity of the rock at its prevailing state of water potential or saturation, in combination with estimates of the hydraulic-head gradient, to directly calculate percolation flux using Darcy's law. Two alcoves were mined into the wall of the north ramp of the Exploratory Studies Facility (ESF) (Figures 1 and 7) 770 m apart. The west dipping north ramp slopes downward through all units of the PTn. Boreholes were drilled in the floor of each alcove and instrumented with heat dissipation probes [*Flint et al.*, 2002a] located to measure the matric potential in the various nonwelded and bedded tuffs. Hydraulic properties were measured on samples collected from the boreholes during drilling.

[41] Volumetric water content was determined with neutron moisture meters and laboratory measurements of core, and the first 5–14 m of the two boreholes showed the effects of evaporation from ventilation in the drift. Flux was calculated using matric potential measurements deeper in the boreholes away from this influence, following equilibration for over a year. Flux was calculated to be downward in the boreholes at rates of ~8–15 mm/yr in the nonwelded PTn and ~1 mm/yr in the underlying Topopah Spring Tuff densely welded rocks. These flux estimates suggest that a significant part of the flux through the PTn is either laterally diverted or converted to fracture flow and therefore does not influence the matric potential of the rock matrix when it reaches the more welded unit below. Calculations of flux along the 6.5-degree slope between the two boreholes resulted in less than 1 mm/yr down dip flux in either the base of the PTn or in the welded top of the Topopah Spring Tuff, supporting the suggestion that most of the water is converted to fracture flow once it penetrates the welded rocks. The uncertainties in this approach include those

**Table 4.** Chloride Concentration (mg/L) for Core Samples From Seven Boreholes Located on the Ridge at Yucca Mountain and Down Dip From the Ridge[a]

| | SD-6 | SD-9 | SD-7 | SD-12 | UZ-7a | NRG-7a | NRG-6 |
|---|---|---|---|---|---|---|---|
| CNW | 43 | | | | | | |
| BT4 | 30 | 170 | | 50 | 70 | | 148 |
| TPY | | 138 | | | | | |
| BT3 | | 93 | 77 | | | 39 | 58 |
| TPP | | 64 | | 46 | | 54 | 62 |
| BT2 | | 40 | | 60 | 74 | | 49 |

[a]Hydrogeologic unit names of the PTn are described in Figure 3.

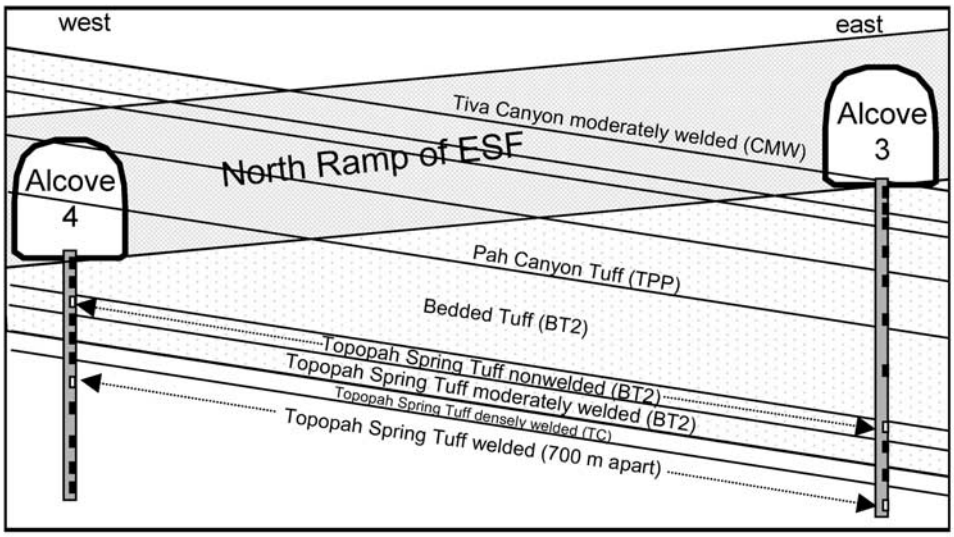


**Figure 7.** Schematic of instrumented boreholes in alcoves 3 and 4 in the North Ramp of the Exploratory Studies Facility (ESF). The North Ramp slopes downward to the west through the eastward sloping beds of the nonwelded rocks of the Paintbrush Group (PTn).

encountered in the measurement of hydraulic conductivities for samples with low saturations, and the calculated fluxes are accurate only within an order of magnitude. Nevertheless, it provides strong indication of a lack of significant lateral diversion down dip over this distance of 700 m. It also provides support for the interpretation of the one-dimensional model results [*Kwicklis et al.*, 1994] that suggest that local spreading occurs in the PTn in locations of concentrated surface runoff or high net infiltration rather than extensive lateral diversion.

[42] A larger-scale evaluation of subsurface distribution of moisture can be used to assess the likelihood of lateral diversion due to the PTn. A comparison of measured matric potential in the Cross Drift (Figure 1) with modeled surface net infiltration (Figure 8) was used to illustrate the apparent lack of significant diversion. Net infiltration is the part of water that crosses the air-surface interface and penetrates deeper than plant roots and evaporation processes and therefore may be assumed to equal percolation flux within the unsaturated zone. Net infiltration is modeled using a water-balance approach, detailed measurements of distributed precipitation, evapotranspiration, and soil and rock water content and properties [*Flint et al.*, 2000]. The comparison is shown for measured matric potential in the Cross Drift with estimated net infiltration at the ground surface along the trace of the Cross Drift (Figure 9). The highest infiltration rate over the Cross Drift is in the PTn where it is exposed at the ground surface on the west side of Yucca Mountain (Figure 2), and is notable in Figure 9 between stations 2200 and 2400. Further west of the exposure of the PTn, the infiltration rate ranges from ~1 to 10 mm/yr and enters the mountain directly in the Topopah Spring Tuff. This yields a rock matric potential in the Cross Drift at station 2450 to 2700 of slightly higher than −0.1 MPa (Figure 9). In this case, there is no overlying PTn and no potential for lateral diversion. The modeled infiltration flux exceeds the saturated hydraulic conductivity of the tuff matrix; therefore fracture flow is dominant and the small fracture/matrix interaction (estimated to be ~0.01% of the total contact area by *Sonnenthal and Bodvarsson* [1999]), and matrix hysteresis does not allow the matrix to come into potential equilibrium with the fractures. This analysis does assume the wetter rock matrix is associated with greater flux through the fracture network. There are many subtleties in Figure 9 that, when evaluated further, may give additional insight into the large-scale mechanisms responsible for subsurface flow. One such subtlety is a shift of lower infiltration (<1 mm/yr) at station 2150 m, which may correspond with the drier rock (>−0.1 MPa) at 1700 m. If the assumption of wetter rock matrix corresponding to greater subsurface flux is correct, this may denote lateral diversion of water that infiltrates above station 1700 down dip, and no diversion of the water that infiltrates to the west of station 2200; thus no flux enters the Topopah Spring Tuff above station 1700. The higher infiltration of >10 mm/yr near station 1700 may correspond to the wetter rock at station 1300. This shift may be due to a 500–600 m of lateral diversion. The overall trend, however, particularly from 0 to 1000 m, shows drier rock under lower infiltration and wetter rock under higher infiltration, suggesting little lateral diversion. There is little or no infiltration west of the end of the Cross Drift because of thick alluvial deposits, so the only water available is water from directly above, further supporting the argument against lateral diversion caused by the PTn.

### 3.2.2. Estimates of Percolation Flux in Topopah Spring Tuff

[43] There are additional lines of evidence supporting vertical flow through the PTn. In an evaluation of large-scale flux processes, if there is a relative similarity between estimates of net infiltration at the ground surface and percolation flux in or below the PTn, it is assumed that the PTn is not diverting a significant part of the percolation water that would ordinarily flow downward through the repository horizon.

[44] In an analysis of methods used to estimate recharge or percolation flux at Yucca Mountain, *Flint et al.* [2002b] describe and show a temperature profile analysis for two

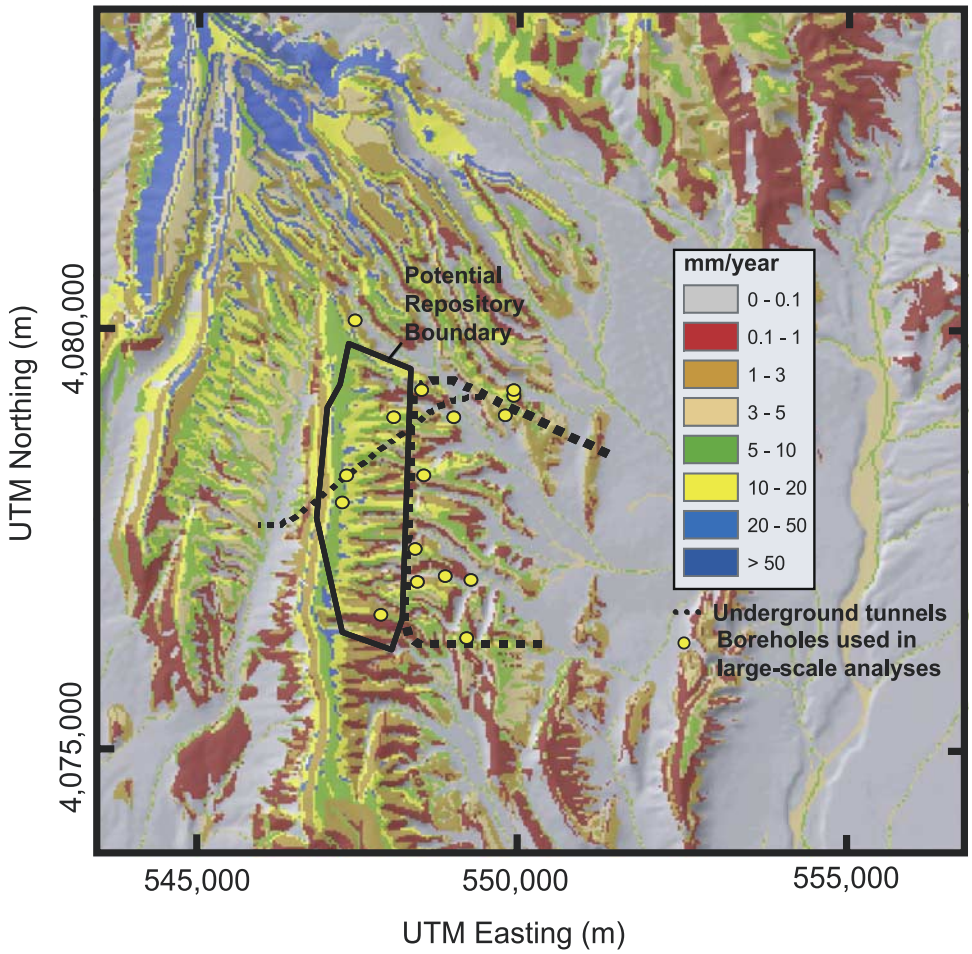


**Figure 8.** Average annual net infiltration spatially distributed at the surface of Yucca Mountain, Nevada, with potential repository boundary, underground tunnels, and boreholes used in large-scale analyses indicated.

boreholes. The temperature profile for a borehole is simulated numerically using measured thermal properties, average annual ground-surface temperatures estimated for each borehole, and measured temperature of the groundwater in the upper part of the saturated zone. The percolation flux for the model is varied to optimize the fit between the measured and simulated temperature profiles. These analyses, conducted on that part of the borehole below the PTn, indicate a

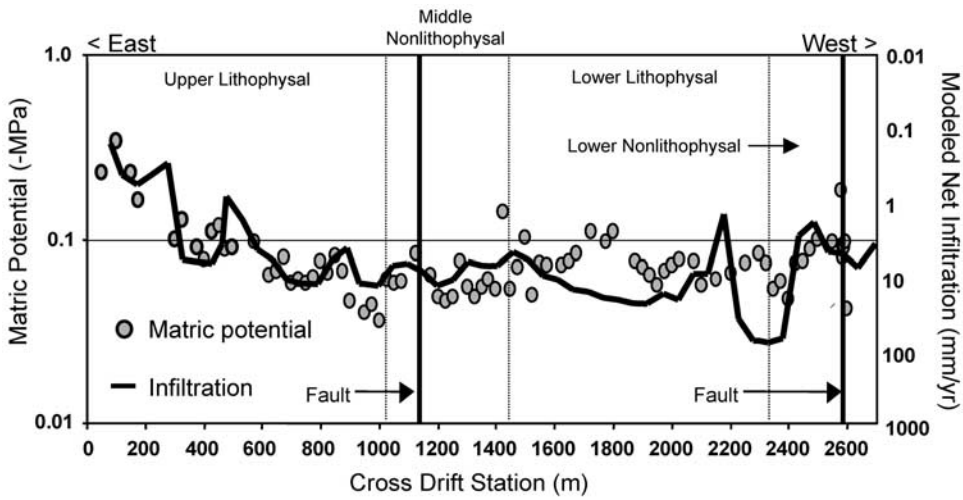


**Figure 9.** Comparison of estimated net infiltration at ground surface with water potential measured subsurface in the Cross Drift.

high flux (~10 mm/yr) directly under the crest of Yucca Mountain for one borehole and a lower flux of less than 1 mm/yr for the borehole to the east of the crest in a wash. These estimates reasonably match the values estimated from the modeled net infiltration for those locations and are shown along with results from eight additional borehole analyses in Figure 10. The estimates of flux generated from modeling temperature profiles somewhat underestimate the flux predicted from the net-infiltration model but are of the same order of magnitude, supporting the similarity in surface and subsurface fluxes.

[45] Estimates of average percolation rate through the unsaturated zone also have been made using pore-water chloride (Cl) concentrations and the chloride-mass-balance method. This method assumes that the flux of Cl deposited at the surface equals the flux of Cl carried through the unsaturated zone by infiltrating water [*Fabryka-Martin et al.*, 1994]. Percolation rates $I$ are estimated from measured Cl concentration using the relationship $I = (PC_o)/C_s$, where $P$ is average annual precipitation; $C_o$ is the effective average Cl concentration in precipitation, including the contribution from dry fallout; and $C_s$ is the measured Cl concentration in subsurface water. The highest percolation rates (4–10 mm/yr) are estimated from data collected in the ESF and the Cross Drift that occur beneath areas with negligible soil cover, such as the ridge tops and side slopes, which is confirmed by surface estimates of net-infiltration flux rate (Figure 11). The lowest percolation rates (0–1 mm/yr) are estimated from samples collected from boreholes in washes with thick alluvium. The flux estimates are from net infiltration simulated on the basis of 30-m grid cells. To capture the increase in scale necessary to compare the surface infiltration with percolation flux in the PTn or Topopah Spring Tuff, the bounds in Figure 11 represent the range of net-infiltration flux over an area surrounding the borehole location of ~200 m in diameter. The samples were collected from the PTn in all of the boreholes and in the North and South Ramps of the ESF, and from the Topopah Spring Tuff in the Main Drift and Cross Drift of the ESF. Estimates of percolation within the PTn that are of the same order of magnitude as those estimated at the ground surface specifically support a lack of diversion because of the upper transition from welded to nonwelded rocks. The calculations of percolation flux using samples from the Topopah Spring Tuff of the repository horizon are also of the same magnitude as that simulated at the surface. The majority of the measurements and calculations of flux in the subsurface using the temperature simulations and CMB calculations support the surface estimates of net infiltration and generally negate a substantial influence of the PTn in diverting water from the repository horizon.

## 4. Summary and Conclusions

[46] On the basis of the field data, interpretations, and calculations above, it seems clear that the early conceptual models of lateral diversion at Yucca Mountain did not take into consideration the scale at which the mechanisms responsible for lateral diversion operate in a natural system. Nor did they consider the range in surface fluxes possible from surface heterogeneities. Neither data nor field observations corroborate the existence of lateral diversion caused by a barrier effect at the bottom of the Tiva Canyon Tuff;

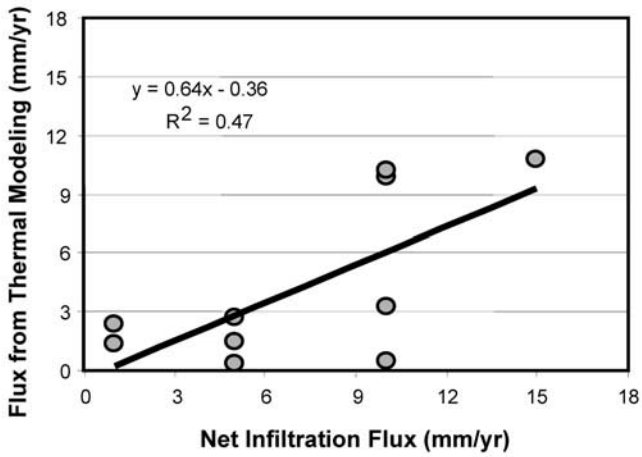


**Figure 10.** Percolation flux simulated from net infiltration model and estimated to simulate measured temperature profiles in several boreholes.

however, observations on the basis of boreholes samples of nearly saturated conditions abruptly declining to <50% saturation supports the possibility of localized barrier effects. The current conceptual model of flow through the PTn describes flow as vertical and slow through the PTn matrix, but there possibly may be local-scale lateral diversion at linear contacts or above low-permeability layers.

### 4.1. Support of Conceptual Model From Calculations

[47] Calculations of the potential for lateral diversion potential do not support significant volumes of diverted water even on the basis of an idealistic representation using mean layer properties. The volume of diverted water is insignificant, and idealized calculation of the maximum lateral distance that water could be diverted is <200 m when system discretization is coarse and <10 m when discretization is fine. None of these estimates approaches the down-dip dimensions of the potential repository, which is ~1000 m. The volumes of diverted water are likely to be even lower when the spatial variability of the properties is considered, as well as the presence of fractures and faults within the hydrogeologic units of the PTn. Additional calculations using Darcy's law made from point data of subsurface water potentials support downward flux in the PTn but suggest that lateral flow over a 700-m distance is less than 1 mm/yr in an area where the overall flux is >5 mm/yr.

[48] These analyses suggest that lateral diversion caused by barriers is a small-scale process and under natural conditions is very unlikely to occur on a large scale, especially in volcanic environments where local heterogeneities, faulting, and fractures predominate. Even apparently uniform ash-flow and ash-fall units have a spatial distribution of hydraulic properties that result in a range of contrasts between adjacent units that limit large-scale capillary barrier mechanisms and permeability barriers to local effects. Because the estimates of diversion are very sensitive to the properties used in calculations of diversion caused by a capillary barrier, the details of the features and properties are necessary to accurately represent and predict these effects. An alternative approach is to stochastically represent the distribution of properties from the mean values and

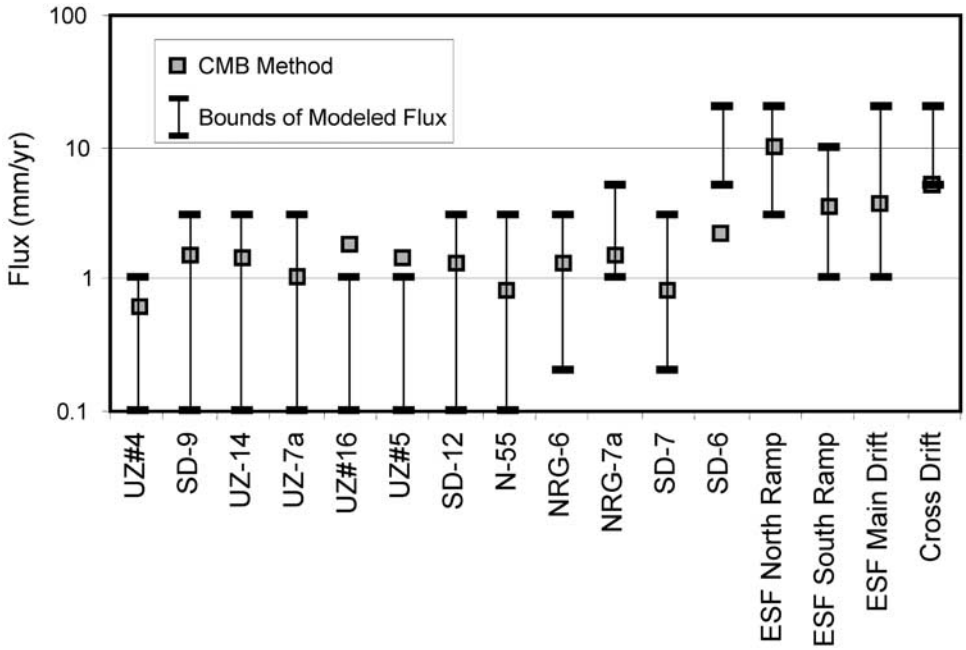


**Figure 11.** Flux calculated using the chloride-mass-balance (CMB) method for 12 boreholes and locations in the Exploratory Studies Facility (ESF) and Cross Drift. All samples are from the PTn, except for those from the ESF Main Drift and the Cross Drift, which are Topopah Spring Tuff.

the variance, and then estimate the range of diversion possible from numerical models.

### 4.2. Evidence for the Lack of Large-Scale Lateral Diversion Caused by PTn

[49] The evaluation of the unsaturated zone at Yucca Mountain has been done using methodologies that represent various spatial scales. Estimates of percolation flux in the Topopah Spring Tuff and other rocks deeper than the PTn generally represent large-scale estimates of flux integrated over large vertical distances. If the early conceptual models of lateral diversion caused by the barrier mechanisms imposed by the PTn were correct, water would be diverted laterally above the repository horizon in the Topopah Spring Tuff and the percolation fluxes would be small in comparison to the fluxes at the ground surface.

[50] An analysis of the distribution of matrix potential in the Cross Drift indicates a general correlation of zones with less negative matric potential and zones with estimates of high net infiltration at the surface. Zones with a more negative matric potential, indicating drier rock, generally corresponded to lower net-infiltration rates. Comparisons of percolation flux estimates using ambient temperatures of deep boreholes, and chloride-mass-balance calculations using data collected in the subsurface in or at depths greater than the PTn, with estimates of surface net infiltration, illustrated similar magnitudes of flux at the surface and below the PTn. These observations support the lack of large-scale diversion caused by the PTn.

[51] There is no one approach, analysis, or data set that provides the necessary support to refute or fully support that lateral diversion occurs above the repository horizon at Yucca Mountain. The combination of analyses and data interpretations of various scales provides evidence to conclude that lateral diversion probably occurs in localized areas, perhaps of the order of meters. However, in addition to the data analyses presented, several other observations provide support for a lack of large-scale diversion. These observations include the spatial variability of matrix properties, which results in discontinuous contrasts at unit interfaces, and the pervasive presence of fractures that obviate the entire capillary barrier process. Diversion is necessarily limited in distance along unit interfaces to the extent that fractures occur in the PTn, or in the rocks above and below the PTn. Although lateral diversion above the repository horizon may occur as a result of permeability barriers at the top and the base of the PTn, the analyses presented that represent large-scale processes provide the same support for generally downward flow. As a result, it would be imprudent to rely on significant lateral diversion to maintain a dry subsurface or reduce the downward percolation of water through the repository horizon.

[52] There are several obvious gaps in the detailed knowledge of information at Yucca Mountain that would be prudent to fill were these processes to be unequivocally assessed. Properties of the fractures at the transitions from welded to nonwelded rocks at the top of the PTn, as well as the transition from the PTn into the TSw, are unknown. It is not known what the distribution of apertures is, or how pervasive the fracture filling is for these locations. Assessments of the lateral heterogeneity of the properties of the PTn did not provide enough details to assess the variability in contrast of hydraulic properties between layers from an analytical perspective and did not address the distribution of fractures penetrating the upper part of the potential barrier at the top of the PTn.

[53] The potential for lateral diversion in natural environments is critical to the understanding of moisture flux and distribution that is required by many scientific investigations, and the application of concepts developed at this site should be broad. The existing state of the knowledge for adequate representation of water flow mechanisms in com-

plex and heterogeneous systems such as fractured rock is nowhere near complete. Theoretical analyses should be pursued to provide accurate and reproducible analytical solutions representing the hydraulic processes in fractured rock, fracture/matrix interaction, and transitions into layers with few fractures. The studies at Yucca Mountain have produced volumes of information, data, and observations to apply to the development of the basic theory and numerical representation of these processes. Although numerical models can be used to further evaluate the role of variable fluxes and the presence of fractures, analytical tools should be developed to address the theory of the transition from matrix flow to fracture flow and subsequent transition from capillary barriers to permeability barriers.

[54] **Acknowledgments.** We thank two reviewers, Benjamin Ross and Edward Kwicklis, as well as two anonymous reviewers, for excellent suggestions for improving the manuscript.

## References

Altman, S. J., B. W. Arnold, R. W. Barnard, G. E. Barr, C. K. Ho, S. A. McKenna, and R. R. Eaton, Flow calculations for Yucca Mountain groundwater travel time (GWTT-95), *Rep. SAND96-0819*, Sandia Natl. Lab., Albuquerque, N. M., 1996.

Buesch, D. C., R. W. Spengler, C. T. Moyer, and J. K. Geslin, Proposed stratigraphic nomenclature and macroscopic identification of lithostratigraphic units of the Paintbrush Group exposed at Yucca Mountain, Nevada, *U.S. Geol. Surv. Open File Rep., 94-469*, 47 pp., 1996.

Civilian Radioactive Waste Management System (CRWMS), Managing and Operations contractor, Analysis of geochemical data for the unsaturated zone, *Rep. ANL-NBS-HS-000017*, Rev 00, Las Vegas, Nev., 2000.

Fabryka-Martin, J. T., S. J. Wightman, B. A. Robinson, and E. W. Vestal, Infiltration processes at Yucca Mountain inferred from chloride and chlorine-36 distributions, *Milestone Rep. 4317*, Los Alamos Natl. Lab., Los Alamos, N. M., 1994.

Fabryka-Martin, J. T., A. L. Flint, D. S. Sweetkind, A. V. Wolfsberg, S. S. Levy, G. J. C. Roemer, J. L. Roach, L. E. Wolfsberg, and M. C. Duff, Evaluation of flow and transport models of Yucca Mountain, based on chlorine-36 and chloride studies for FY97, *Yucca Mt. Proj. Milestone Rep. SP2224M3*, Los Alamos Natl. Lab., Los Alamos, N. M., 1997.

Flint, L. E., Characterization of hydrogeologic units using matrix properties, *U.S. Geol. Surv. Water Resour. Invest. Rep., 96-4342*, 61 pp., 1998.

Flint, L. E., Characterization of unsaturated zone hydrologic properties and their influence on lateral diversion in a volcanic tuff at Yucca Mountain, Nevada, Ph.D. dissertation, 161 pp., Oreg. State Univ., Corvallis, 2002.

Flint, L. E., and A. L. Flint, Distribution of water potential measured with heat dissipation probes in underground volcanic tuffs, paper presented at the Geological Society of America Annual Meeting, Reno, Nev., Nov. 2000.

Flint, L. E., A. L. Flint, C. A. Rautman, and J. D. Istok, Physical and hydrologic properties of rock outcrop samples at Yucca Mountain, Nevada, *U.S. Geol. Surv. Open File Rep., 95-280*, 70 pp., 1996.

Flint, A. L., L. E. Flint, J. A. Hevesi, D'F. A. Agnese, and C. C. Faunt, Estimation of recharge and travel-time through the unsaturated zone in arid climates, in *Dynamics of Fluids in Fractured Rock*, *Geophys. Monogr. Ser.*, vol. 122, edited by B. Faybishenko, P. Witherspoon, and S. Benson, pp. 115–128, AGU, Washington, D. C., 2000.

Flint, A. L., L. E. Flint, G. S. Bodvarsson, E. M. Kwicklis, and J. T. Fabryka-Martin, Evolution of the conceptual model of vadose zone hydrology for Yucca Mountain, *J. Hydrol.*, *247*(1–2), 1–30, 2001a.

Flint, A. L., L. E. Flint, E. M. Kwicklis, G. S. Bodvarsson, and J. T. Fabryka-Martin, Hydrology of Yucca Mountain, *Rev. Geophys.*, *39*(4), 447–470, 2001b.

Flint, A. L., G. S. Campbell, K. M. Ellett, and C. Calissendorff, Calibration and temperature correction of heat dissipation matric potential sensors, *Soil Sci. Soc. Am. J.*, *66*, 1439–1445, 2002a.

Flint, A. L., L. E. Flint, E. M. Kwicklis, J. T. Fabryka-Martin, and G. S. Bodvarsson, Estimating recharge at Yucca Mountain, Nevada, USA: Comparison of methods, *Hydrogeol. J.*, *10*, 180–204, 2002b.

Gardner, W. R., Some steady-state solutions of the unsaturated moisture flow equation with application to evaporation from a water table, *Soil Sci.*, *86*, 228–232, 1958.

Heiberger, T. S., Simulating the effects of a capillary barrier using the two-dimensional variably saturated flow model SWMS-2D/HYDRUS-2D, Master's thesis, 124 pp., Oreg. State Univ., Corvallis, 1996.

Hevesi, J. A., A. L. Flint, and J. D. Istok, Precipitation estimation in mountainous terrain using multivariate geostatistics, II, Isohyetal maps, *J. Appl. Meteorol.*, *31*(7), 677–688, 1992.

Ho, C. K., Assessing alternative conceptual models of fracture flow, in *TOUGH Workshop >95, Proceedings*, edited by K. Pruess, *Rep. LBL-37200*, Lawrence Berkeley Natl. Lab., Berkeley, Calif., 1995.

Ho, C. K., and S. W. Webb, Capillary barrier performance in heterogeneous porous media, *Water Resour. Res.*, *34*(4), 603–609, 1998.

Istok, J. D., C. A. Rautman, L. E. Flint, and A. L. Flint, Spatial variability in hydrologic properties of a volcanic tuff, *Ground Water*, *32*, 751–760, 1994.

Klavetter, E. A., and R. R. Peters, Estimation of hydrologic properties of an unsaturated fractured rock mass, *Rep. SAND84-2642*, Sandia Natl. Lab., Albuquerque, N. M., 1986.

Kwicklis, E. M., and R. W. Healy, Numerical investigation of steady liquid water flow in a variably saturated fracture network, *Water Resour. Res.*, *29*(12), 4091–4102, 1993.

Kwicklis, E. M., A. L. Flint, and R. W. Healy, Simulation of flow in the unsaturated zone beneath Pagany Wash, Yucca Mountain, in *Proceedings of the 5th International High-Level Radioactive Waste Manage Conference, May 22–26, Las Vegas, Nevada*, pp. 2341–2351, Am. Nucl. Soc., La Grange Park, Ill., 1994.

Montazer, P., and W. E. Wilson, Conceptual hydrologic model of flow in the unsaturated zone, Yucca Mountain, Nevada, *U.S. Geol. Surv. Water Resour. Invest. Rep., 84-4345*, 55 pp., 1984.

Moyer, T. C., J. K. Geslin, and L. E. Flint, Stratigraphic relations and hydrologic properties of the Paintbrush Tuff nonwelded (PTn) hydrologic unit, Yucca Mountain, Nevada, *U.S. Geol. Surv. Open File Rep., 95-397*, 151 pp., 1996.

Peters, R. R., and E. A. Klavetter, A continuum model for water movement in an unsaturated fractured rock mass, *Water Resour. Res.*, *24*(3), 416–430, 1988.

Rautman, C. A., and A. L. Flint, Deterministic processes and stochastic modeling, in *Proceedings of the 2nd Annual International High-Level Radioactive-Waste Management Conference*, pp. 1617–1624, Am. Nucl. Soc., La Grange Park, Ill., 1992.

Ritcey, A. C., and Y. S. Wu, Evaluation of the effect of future climate change on the distribution and movement of moisture in the unsaturated zone at Yucca Mountain, Nevada, *J. Contam. Hydrol.*, *38*, 257–279, 1999.

Rockhold, M. L., B. Sagar, and M. P. Connelly, Multidimensional modeling of unsaturated flow in the vicinity of exploratory shafts and fault zones at Yucca Mountain, Nevada, in *First International High Level Radioactive Waste Management Conference, Las Vegas, Nevada, Proceedings*, pp. 153–162, Am. Nucl. Soc., La Grange Park, Ill., 1990.

Roseboom, E. H., Jr., Disposal of high-level nuclear waste above the water table in arid regions, *Geol. Surv. Circ.*, *903*, 21 pp., 1983.

Ross, B., The diversion capacity of capillary barriers, *Water Resour. Res.*, *26*(10), 2625–2629, 1990.

Rulon, J. J., G. S. Bodvarsson, and P. Montazer, Preliminary numerical simulations of groundwater flow in the unsaturated zone, Yucca Mountain, Nevada, *Rep. LBL 20553*, 91 pp., Lawrence Berkeley Natl. Lab., Berkeley, Calif., 1986.

Scott, R. B., R. W. Spengler, S. Diehl, A. R. Lappin, and M. P. Chornack, Geologic character of tuffs in the unsaturated zone at Yucca Mountain, southern Nevada, in *Role of the Unsaturated Zone in Radioactive and Hazardous Waste Disposal*, edited by J. W. Mercer, P. S. C. Rao, and I. W. Marine, pp. 289–335, Ann Arbor Sci., Ann Arbor, Mich., 1983.

Selker, J. S., C. K. Keller, and J. R. McCord, *Vadose Zone Processes*, 339 pp., CRC Press, Boca Raton, Fla., 1999.

Sinnock, S., Y. T. Lin, and J. P. Brannen, Preliminary bounds on the expected post-closure performance of the Yucca Mountain repository site, southern Nevada, *J. Geophys. Res.*, *92*(B8), 7820–7842, 1987.

Sonnenthal, E. L., and G. S. Bodvarsson, Constraints on the hydrology of the unsaturated zone at Yucca Mountain, Nevada, from three-dimensional models of chloride and strontium geochemistry, *J. Contam. Hydrol.*, *38*(1–3), 107–157, 1999.

Steenhuis, T. S., J. Y. Parlange, and K.-J. S. Kung, Comment on "The diversion capacity of capillary barriers" by Benjamin Ross, *Water Resour. Res.*, *27*(8), 2155–2156, 1991.

van Genuchten, M. T., A closed-form equation for predicting the hydraulic conductivity of unsaturated soils, *Soil Sci. Soc. Am. J.*, *44*, 892–898, 1980.

Walter, M. T., J.-S. Kim, T. S. Steenhuis, J.-Y. Parlange, A. Heilig, R. D. Braddock, J. S. Selker, and J. Boll, Funneled flow mechanisms in a sloping layered soil: Laboratory investigation, *Water Resour. Res.*, *36*(4), 841–849, 2000.

Wilson, M. L., Lateral diversion in the PTn unit: Capillary-barrier analysis, in *Sixth International High Level Radioactive Waste Management Conference, Las Vegas, Nevada, Proceedings*, Am. Nucl. Soc., La Grange Park, Ill., 1996.

Winograd, I. J., Radioactive waste disposal in thick unsaturated zones, *Science*, *212*(4502), 1457–1464, 1981.

A. L. Flint and L. E. Flint, Water Resources Division, U.S. Geological Survey, Placer Hall, 6000 J Street, Sacramento, CA 95819-6129, USA. (lflint@usgs.gov)

J. S. Selker, Department of Bioresource Engineering, University of Oregon, Corvallis, OR 97330, USA.